Supplemental Materials and Methods

Generation of FGF19+ BAC transgenic mouse

FAH$^{-/-}$Rag2$^{-/-}$Il2rg$^{-/-}$NOD$^{-/-}$ ("FRGN") female mice of 3 weeks' age were superovulated via standard intraperitoneal (IP) injection of 5 IU PMSG (Pregnant Mare Serum Gonadotropin) on Day -3, followed on Day -1 with IP injection of 5 IU HCG (Human Chorionic Gonadotropin), and mated with FRGN males on Day 0. Females where checked for vaginal plugs, and those with plugs were sacrificed on Day 0.5 or Day 1, and fertilized oocytes (zygotes) collected. Sixty FRGN zygotes where injected with the FGF19+ BAC vector (1 ug/mL)[1] and implanted into surrogate immune competent mice. Twelve pups were born, of which four harbored the transgene, one of which was used to start the FGF19+ colony.

Assessment of non-FGF19 effects of BAC transgene

Two coding regions (other than FGF19) reside in the BAC transgene, genes CCND1 and ORAOV1 (Fig. S1c). Figure S1d shows the regulation of all three BAC-inserted genes in various conditions. Note that the genes are differentially regulated, suggesting that regulatory elements within the BAC allow for physiologic regulation of these genes similar to FGF19. Also note that in the livers of human hepatocyte repopulated mice, those without the BAC transgene do not express FGF19, but do express gene products of CCND1 and ORAOV1, while mice with the BAC express FGF19, CCND1 and ORAOV1. The latter two gene products are expressed at lower levels compared to the non-transgenic mice, suggesting the BAC does not lead to disregulated expression of these genes.

Bile duct ligation and bile acid infusion

For the bile duct ligation (BDL), 8 week-old male mice were anesthetized with isoflurane. After laparotomy, the common bile duct was ligated with two sutures then cut between the sutures, and the abdomen closed. Animals were killed after 7 days and tissues collected for analysis.

For the bile acid infusion model, 8-12 week old male mice were anesthetized with isoflurane. A small catheter (MRE10, Braintree, O.D. = 0.010") was introduced into the portal vein such that portal flow was not compromised. The small catheter was attached to a larger catheter (MRE40, O.D. = 0.040"), externalized, and connected to an infusion pump. The

catheter was protected by a spring tether mounted to a lever-arm on a special cage designed for infusions (Harvard Apparatus), allowing mice free movement in the cage and normal access to food and water. Portal vein infusions ran at 200 uL per hour, and contained either 0.9% saline (control) or 0.025M Na Taurocholate (Sigma) dissolved in 0.9% saline, and ran for 24 or 48 hours prior to sacrifice.

Intestinal bile acid pool analysis

Intestines and intestinal contents were collected (between stomach and cecum). The intestines and contents were homogenized in a 5% KOH/95% ethanol solution by heating at 70 C for 4 hours. After subsequent removal of particulate matter, the remaining solution was analyzed for total bile acids using an enzymatic Total Bile Acids Test Kit (Diazyme) and normalizing to animal weight.

Tissue analysis

Liver, intestine and serum were snap frozen in liquid nitrogen when animals were killed; some liver was fixed in formalin for immunohistochemistry. Body weights were measured immediately prior to killing the mice, and liver weights determined immediately after explantation. Serum FGF 19 levels, quantitative real-time RT-PCR (qPCR) and complete RNA sequencing were performed as noted.

Quantitative real-time RT-PCR (qPCR)

RNA was isolated, reverse transcribed, and measured by real-time reverse transcriptase–PCR using SYBR green as previously described.[2] (Life Technologies, Carlsbad, CA) (primers are listed in **Supplemental Table 1**).

Histology

Mouse liver was immersed in 4% formalin immediate after collection, embedded in paraffin, and slides cut in the usual fashion. Staining for FAH was performed using a polyclonal rabbit FAH antibody (Lucie Germain, Ph.D., Laval University), followed by use of anti-rabbit ImmPRESS polymer (Vector Laboratories), with AEC used as the chromogen. Routine hematoxylin and eosin staining was done for all samples, while separate slides were used for FAH staining.

Complete RNA sequencing

Sequencing libraries were constructed using the Illumina TruSeq RNAseq kit. Briefly, poly(A)+ RNA was isolated from total RNA using oligo-dT coated magnetic beads. The recovered RNA was then chemically fragmented. First strand cDNA was generated using random hexamers as primers for reverse transcriptase. Following second strand synthesis, the ends of the double stranded fragments were repaired and then a single "A" nucleotide was added to each end. Illumina adaptors were ligated to the cDNAs. Limited round PCR was used to amplify the material to yield the final library. Library concentration was determined using real time PCR with primers complementary to the Illumina adaptors. Sample libraries were diluted and applied to an Illumina paired end flow cell at a concentration appropriate to generate about 180 million reads per lane. All libraries were prepared with indexing barcodes to permit multiplex runs. 50 cycle single read sequencing were used to generate base call files. Illumina's CASAVA package was used to assemble the reads into standard fastq formatted data.

RNA sequencing gene set analysis

Raw fastq data from RNA libraries was transformed into Reads Per Kilobase Million (RPKM), which allows a normalized comparison between libraries. RPKM data was analyzed using Gene Set Enrichment Analysis (GSEA) as described.[3] Heatmaps and hierarchical clustering used GENE-E (http://www.broadinstitute.org/cancer/software/GENE-E/index.html). Gene set constituents are noted in **Supplemental Table 2**). Differences in gene sets were considered significant if the false discovery rate (FDR) qvalue was < 0.05, a more stringent statistic than the p value. All differences between gene sets with an FDR qvalue < 0.05 also had p values < 0.05. Complete RNA sequencing data can be found at the NCBI GEO website, SRA198069 , "FGF19 signaling controls liver size."

Serum and bile FGF19 measurements

Serum and bile FGF19 concentrations were performed in triplicate with an ELISA according to the manufacturer's instructions (FGF-19 Omnikine ELISA, Assay Biotechnology). Serum ALT levels were assayed in triplicate with an ALT (SGPT) Reagent Kit (Color Endpoint) (Bio-quant, Cat # BQ 004A-CR).

Flow cytometry methods for isolating biliary ductal cells

A piece of human liver explant taken from a patient undergoing liver transplant for biliary cirrhosis due to biliary atresia was perfused with EBSS (Gibco, CA) with 1mM EGTA (Fisher Chemical, NJ) and then collagenase type2 (Worthington, NJ). Hepatocytes were depleted with a spin of 800rpm for 3min. Supernatant was spun at a speed of 1400rpm for 5min, non-parenchymal cells (NPCs) were included in the pellets. Cells were incubated at 4°C for 20 minutes with FITC conjugated anti-DHIC5-4D9, APC-H7 CD45 (BD Pharmingen, CA) and APC-H7 CD14 (BD Pharmingen), Alexa 647 anti- CD31 (BD Pharmingen). Cells were washed 3 times and resuspended in staining medium containing propidium iodide (1 µg/mL) (Sigma, St Louis, MO). Labeled cells were analyzed and separated with BD Influx sorter (BD Biosciences, CA) and Flowjo software (Flowjo, OR). After removal of doublets with trigger pulse width, PI^+ dead cells, hematopoietic cells, macrophages and endothelial cells by CD45 CD14 and CD31 antibodies, ductal cells are purified in this cell fraction: $DHIC5\text{-}4D9^+CD45^-CD14^-CD31^-$.

Note that our lab uses the DHIC5-4D9/HPd3 antibody as a pan-ductal marker.[4] DHIC5-4D9/HPd3 co-labels cells staining for Keratin 19, another common bile duct marker.

References

1. Schedl, A., *et al.* A method for the generation of YAC transgenic mice by pronuclear microinjection. *Nucleic Acids Res* **21,** 4783-4787 (1993).
2. Madison, B.B., *et al.* Cis elements of the villin gene control expression in restricted domains of the vertical (crypt) and horizontal (duodenum, cecum) axes of the intestine. *J Biol Chem* **277,** 33275-33283 (2002).
3. Subramanian, A., *et al.* Gene set enrichment analysis: a knowledge-based approach for interpreting genome-wide expression profiles. *Proc Natl Acad Sci U S A* **102,** 15545-15550 (2005).
4. Dorrell, C., *et al.* Transcriptomes of the major human pancreatic cell types. *Diabetologia* **54,** 2832-2844 (2011).

Supplemental Tables and Figures

Supplemental Table 1 PCR Primer List

qPCR primer	**Sequence (5′-3′)**
Mouse Cyp7a F (for qRT-PCR)	TGGAATAAGGAGAAGGAAAGTA
Mouse Cyp7a R (for qRT-PCR)	TGTGTCCAAATGCCTTCGCAGA
Mouse FGF15 F (for qRT-PCR)	GAGGACCAAAACGAACGAAATT
Mouse FGF15 R (for qRT-PCR)	ACGTCCTTGATGGCAATCG
Mouse Gapdh F (for qRT-PCR)	CGACTTCAACAGCAACTC
Mouse Gapdh R (for qRT-PCR)	GTAGCCGTATTCATTGTCAT
Mouse Fgf15 F (for qRT-PCR)	GAGGACCAAAACGAACGAAATT
Mouse Fgf15 R (for qRT-PCR)	ACGTCCTTGATGGCAATCG
Human FGF19 F (for qRT-PCR)	CACGGGCTCTCCAGCTGCTTCCTGCG
Human FGF19 R (for qRT-PCR)	TCCTCCTCGAAAGCACAGTCTTCCTCCG
Human FGF19 F (Genomic 3′ end)	CCAAACAGCGCGGGACGCTAG
Human FGF19 R (Genomic 3′ end)	AAGGCCCGAGGTGGGTTTTCCT
Human FGF19 F (Genomic 5′ end)	TCCTCCCGTGGACGGTGCT
Human FGF19 R (Genomic 5′ end)	AGGCATGGCCCACCAGGCTT
Human Lamin F (for qRT-PCR)	CCTCCTCGCCCTCCAAGAGC
Human Lamin R (for qRT-PCR)	AGATGCGGGCAAGGATGCAG
Human CYP7A F (for qRT-PCR)	TGGATTAGGAGAAGGCAAACG
Human CYP7A R (for qRT-PCR)	TGTGCCCAAATGCCTTCGCAGA

Supplemental Table 2 Gene set constituents

Hippo Signaling	**Bile acid Synthesis**	**Cholestasis Pathway**	**FGFR4 Ligand**
AMOT	ABCB11	ABCB11	FGF1
AMOTL1	ACOT8	ABCC2	FGF17
AMOTL2	ACOX2	ABCC3	FGF18
CASP3	AKR1C4	ABCC4	FGF19
CCND1	AKR1D1	ALB	FGF2
CTGF	AMACR	BAAT	FGF20
DIAPH1	BAAT	FABP6	FGF23
DVL2	CH25H	SLC10A1	FGF4
LATS1	CYP27A1	SLC10A2	FGF6
LATS2	CYP39A1	SLC27A5	FGF8
NPHP4	CYP46A1	SLCO1A2	FGF9
SAV1	CYP7A1	SLCO1B1	FGFR4
STK3	CYP7B1	SLCO1B3	
STK4	CYP8B1		
TEAD1	HSD17B4		
TJP1	HSD3B7		
TJP2	SCP2		
WWC1	SLC27A2		
WWTR1	SLC27A5		
YAP1			
YWHAB			
YWHAE			

Supplemental Table 2 Gene set constituents

DNA Replication

AHCTF1	CENPC1	GINS2	MCM6	PMF1	PSMA4	PSMD12	RPA1
APITD1	CENPH	GINS4	MCM7	POLA1	PSMA5	PSMD13	RPA2
AURKB	CENPI	GMNN	MCM8	POLA2	PSMA6	PSMD14	RPA3
B9D2	CENPK	GORASP1	MIS12	POLD1	PSMA7	PSMD2	RPA4
BIRC5	CENPL	INCENP	MLF1IP	POLD2	PSMA8	PSMD3	RPS27
BUB1	CENPM	ITGB3BP	NDC80	POLD3	PSMB1	PSMD4	RPS27A
BUB1B	CENPN	KIF18A	NDEL1	POLD4	PSMB10	PSMD5	RPS27AP11
BUB3	CENPO	KIF20A	NSL1	POLE	PSMB2	PSMD6	SEC13
CASC5	CENPP	KIF23	NUDC	POLE2	PSMB3	PSMD7	SEH1L
CCDC99	CENPQ	KIF2A	NUF2	PPP1CC	PSMB4	PSMD8	SGOL1
CCNA1	CENPT	KIF2B	NUP107	PPP2CA	PSMB5	PSMD9	SGOL2
CCNA2	CKAP5	KIF2C	NUP133	PPP2CB	PSMB6	PSME1	SKA1
CDC20	CLASP1	KNTC1	NUP37	PPP2R1A	PSMB7	PSME2	SKA2
CDC45	CLIP1	LIG1	NUP43	PPP2R1B	PSMB8	PSME4	SKA2L
CDC6	DBF4	LOC645084	NUP85	PPP2R5A	PSMB9	PSMF1	SMC1A
CDC7	DNA2	LOC652826	ORC1	PPP2R5B	PSMC1	RAD21	SMC3
CDCA8	DSN1	MAD1L1	ORC2	PPP2R5C	PSMC2	RANBP2	SPC24
CDK2	E2F1	MAD2L1	ORC3	PPP2R5D	PSMC3	RANGAP1	SPC25
CDKN1A	E2F2	MAPRE1	ORC4	PPP2R5E	PSMC4	RB1	STAG1
CDKN1B	E2F3	MCM10	ORC5	PRIM1	PSMC5	RCC2	STAG2
CDT1	ERCC6L	MCM2	ORC6	PRIM2	PSMC6	RFC2	TAOK1
CENPA	FBXO5	MCM3	PAFAH1B1	PSMA1	PSMD1	RFC3	UBA52
CENPC1	FEN1	MCM4	PCNA	PSMA2	PSMD10	RFC4	XPO1
CENPH	GINS1	MCM5	PLK1	PSMA3	PSMD11	RFC5	ZW10
							ZWILCH
							ZWINT

Supplemental Table 2 Gene set constituents

Apoptosis

ACIN1	CASP9	FNTA	PLEC	PSMC2	RIPK1
ADD1	CDH1	GAS2	PMAIP1	PSMC3	ROCK1
AKT1	CFLAR	GSN	PPP3R1	PSMC4	RPS27A
APAF1	CTNNB1	GZMB	PRKCD	PSMC5	SATB1
APC	CYCS	H1F0	PRKCQ	PSMC6	SPTAN1
APPL1	DAPK1	HIST1H1A	PSMA1	PSMD1	STK24
ARHGAP10	DAPK2	HIST1H1B	PSMA2	PSMD10	TFDP1
BAD	DAPK3	HIST1H1C	PSMA3	PSMD11	TJP1
BAK1	DBNL	HIST1H1D	PSMA4	PSMD12	TJP2
BAX	DCC	HIST1H1E	PSMA5	PSMD13	TNF
BBC3	DFFA	HMGB1	PSMA6	PSMD14	TNFRSF10B
BCAP31	DFFB	HMGB2	PSMA7	PSMD2	TNFRSF1A
BCL2	DIABLO	KPNA1	PSMA8	PSMD3	TNFSF10
BCL2L1	DNM1L	KPNB1	PSMB1	PSMD4	TP53
BCL2L11	DSG1	LMNA	PSMB10	PSMD5	TRADD
BID	DSG2	LMNB1	PSMB2	PSMD6	TRAF2
BIRC2	DSG3	MAGED1	PSMB3	PSMD7	UBA52
BMF	DSP	MAPK8	PSMB4	PSMD8	UNC5A
BMX	DYNLL1	MAPT	PSMB5	PSMD9	UNC5B
CASP10	DYNLL2	MST4	PSMB6	PSME1	VIM
CASP3	E2F1	NMT1	PSMB7	PSME2	XIAP
CASP6	FADD	OCLN	PSMB8	PSME4	YWHAB
CASP7	FAS	PAK2	PSMB9	PSMF1	
CASP8	FASLG	PKP1	PSMC1	PTK2	

Supplemental Table 2 Gene set constituents

Cell Cycle

ACD	CDC20	CEP250	GINS1	HIST2H2AA3	MCM8	POLE2	PSMC5	RPA2	TFDP1
ACTR1A	CDC23	CEP290	GINS2	HIST2H2AA4	MDM2	POT1	PSMC6	RPA3	TINF2
AHCTF1	CDC25A	CEP57	GINS4	HIST2H2AC	MIS12	PPP1CC	PSMD1	RPA4	TK2
AKAP9	CDC25B	CEP63	GMNN	HIST2H2BE	MLF1IP	PPP2CA	PSMD10	RPS27	TP53
ALMS1	CDC25C	CEP70	GORASP1	HIST2H4A	MNAT1	PPP2CB	PSMD11	RPS27A	TUBA1A
ANAPC1	CDC26	CEP72	H2AFX	HIST2H4B	MYBL2	PPP2R1A	PSMD12	RRM2	TUBA4A
ANAPC10	CDC27	CEP76	H2AFZ	HIST3H2BB	MYC	PPP2R1B	PSMD13	RSF1	TUBB
ANAPC11	CDC45	CETN2	HAUS2	HIST3H3	NDC80	PPP2R2A	PSMD14	RUVBL1	TUBG1
ANAPC2	CDC6	CHEK1	HDAC1	HIST4H4	NDEL1	PPP2R3B	PSMD2	RUVBL2	TUBG2
ANAPC4	CDC7	CHEK2	HIST1H2AB	HJURP	NEDD1	PPP2R5A	PSMD3	SDCCAG8	TUBGCP2
ANAPC5	CDCA8	CKAP5	HIST1H2AC	HSP90AA1	NEK2	PPP2R5B	PSMD4	SEC13	TUBGCP3
ANAPC7	CDK1	CKS1B	HIST1H2AD	HSPA2	NHP2	PPP2R5C	PSMD5	SEH1L	TUBGCP5
APITD1	CDK2	CLASP1	HIST1H2AE	HUS1	NINL	PPP2R5D	PSMD6	SGOL1	TUBGCP6
ATM	CDK4	CLIP1	HIST1H2AJ	INCENP	NPM1	PPP2R5E	PSMD7	SGOL2	TYMS
ATR	CDK5RAP2	CSNK1D	HIST1H2BA	ITGB3BP	NSL1	PRIM1	PSMD8	SKA1	UBA52
ATRIP	CDK6	CSNK1E	HIST1H2BB	KIF18A	NUDC	PRIM2	PSMD9	SKA2	UBE2C
AURKA	CDK7	CUL1	HIST1H2BC	KIF20A	NUF2	PRKACA	PSME1	SKP1	UBE2D1
AURKB	CDKN1A	DBF4	HIST1H2BD	KIF23	NUMA1	PRKAR2B	PSME2	SKP2	UBE2E1
AZI1	CDKN1B	DCTN1	HIST1H2BE	KIF2A	NUP107	PSMA1	PSME4	SMARCA5	UBE2I
B9D2	CDKN2A	DCTN2	HIST1H2BF	KIF2B	NUP133	PSMA2	PSMF1	SMC1A	WEE1
BIRC5	CDKN2B	DCTN3	HIST1H2BG	KIF2C	NUP37	PSMA3	PTTG1	SMC1B	WRAP53
BRCA1	CDKN2C	DHFR	HIST1H2BH	KNTC1	NUP43	PSMA4	RAD1	SMC3	XPO1
BTRC	CDKN2D	DIDO1	HIST1H2BI	LIG1	NUP85	PSMA5	RAD17	SPC24	YWHAE
BUB1	CDT1	DKC1	HIST1H2BJ	LIN37	OFD1	PSMA6	RAD21	SPC25	YWHAG
BUB1B	CENPA	DNA2	HIST1H2BK	LIN52	OIP5	PSMA7	RAD9A	SSNA1	ZW10
BUB3	CENPC1	DSN1	HIST1H2BL	LIN54	PAFAH1B1	PSMA8	RANBP2	STAG1	ZWILCH
CASC5	CENPH	DYNC1H1	HIST1H2BM	LIN9	PCM1	PSMB1	RANGAP1	STAG2	ZWINT
CCDC99	CENPI	DYNC1I2	HIST1H2BN	LMNA	PCNA	PSMB10	RB1	STAG3	
CCNA1	CENPJ	DYNLL1	HIST1H2BO	LMNB1	PCNT	PSMB2	RBBP4	SUN2	
CCNA2	CENPK	DYRK1A	HIST1H4A	MAD1L1	PKMYT1	PSMB3	RBBP7	SYCP1	
CCNB1	CENPL	E2F1	HIST1H4B	MAD2L1	PLK1	PSMB4	RBL1	SYCP2	
CCNB2	CENPM	E2F2	HIST1H4C	MAPRE1	PLK4	PSMB5	RBL2	SYCP3	
CCND1	CENPN	E2F3	HIST1H4D	MAX	PMF1	PSMB6	RCC2	SYNE1	
CCND2	CENPO	E2F4	HIST1H4E	MCM10	POLA1	PSMB7	REC8	SYNE2	
CCND3	CENPP	E2F5	HIST1H4F	MCM2	POLA2	PSMB8	RFC2	TAOK1	
CCNE1	CENPQ	ERCC6L	HIST1H4H	MCM3	POLD1	PSMB9	RFC3	TERF1	
CCNE2	CENPT	FBXO5	HIST1H4I	MCM4	POLD2	PSMC1	RFC4	TERF2	
CCNH	CEP135	FEN1	HIST1H4J	MCM5	POLD3	PSMC2	RFC5	TERF2IP	
CDC14A	CEP164	FGFR1OP	HIST1H4K	MCM6	POLD4	PSMC3	RFWD2	TERT	
CDC16	CEP192	FKBP6	HIST1H4L	MCM7	POLE	PSMC4	RPA1	TEX12	

Supplemental Table 2 Gene set constituents

FOXM1 Pathway		**WNT Signaling**	**IL6 Pathway**	**PTEN Signaling**
AURKB	HIST1H2BA	APC	CEBPB	AKT1
BIRC5	LAMA4	AXIN1	CSNK2A1	BCAR1
BRCA2	MAP2K1	BTRC	ELK1	CDKN1B
CCNA2	MMP2	CCND1	FOS	FASLG
CCNB1	MYC	CREBBP	GRB2	FOXO3
CCNB2	NEK2	CSNK1A1	HRAS	GRB2
CCND1	NFATC3	CSNK1D	IL6	ILK
CCNE1	ONECUT1	CSNK2A1	IL6R	ITGB1
CDC25B	PLK1	CTBP1	IL6ST	MAPK1
CDK1	RB1	CTNNB1	JAK1	MAPK3
CDK2	SKP2	DVL1	JAK2	PDK2
CDK4	SP1	FRAT1	JAK3	PDPK1
CDKN2A	TGFA	FZD1	JUN	PIK3CA
CENPA	XRCC1	GSK3B	MAP2K1	PIK3R1
CENPB		HDAC1	MAPK3	PTEN
CENPF		LEF1	PTPN11	PTK2
CHEK2		MAP3K7	RAF1	SHC1
CKS1B		MYC	SHC1	SOS1
CREBBP		NLK	SOS1	
EP300		PPARD	SRF	
ESR1		PPP2CA	STAT3	
ETV5		SMAD4	TYK2	
FOS		TAB1		
FOXM1		TLE1		
GAS1		WIF1		
GSK3A		WNT1		

Supplemental Table 2 Gene set constituents

MYC		**MET**	
Pathway		**Pathway**	
ACTL6A	MYC	AKT1	MTOR
BAX	MYCT1	AKT1S1	MUC20
BCAT1	NBN	AKT2	NCK1
BIRC5	NCL	APC	NCK2
BMI1	NDUFAF2	ARF6	NUMB
CAD	NME1	ARHGEF4	PAK1
CCNB1	NME2	BAD	PAK2
CCND2	NPM1	BCAR1	PAK4
CDC25A	ODC1	CBL	PARD6A
CDCA7	PDCD10	CDC42	PDPK1
CDK4	PEG10	CDH1	PIK3CA
CREBBP	PFKM	CRK	PIK3R1
DDX18	PIM1	CRKL	PLCG1
E2F3	PMAIP1	CTNNA1	PRKCI
EIF2S1	POLR3D	CTNNB1	PRKCZ
EIF4A1	PRDX3	EGR1	PTK2
EIF4E	PTMA	EIF4E	PTPN1
EIF4G1	RCC1	EIF4EBP1	PTPN11
ENO1	RPL11	EPS15	PTPN2
EP300	RUVBL1	ETS1	PTPRJ
FOSL1	RUVBL2	F2RL2	PXN
GAPDH	SERPINI1	GAB1	RAB5A
GPAM	SHMT1	GAB2	RAC1
HMGA1	SLC2A1	GRB2	RAF1
HSP90AA1	SMAD3	HGF	RANBP10
HSPA4	SMAD4	HGS	RANBP9
HSPD1	SNAI1	HRAS	RAP1A
HUWE1	SUPT3H	INPP5D	RAP1B
ID2	SUPT7L	INPPL1	RAPGEF1
IREB2	TAF10	JUN	RHOA
KAT2A	TAF12	KPNB1	RIN2
KAT5	TAF4B	MAP2K1	RPTOR
KIR3DL1	TAF9	MAP2K2	SH3GL2
LDHA	TERT	MAP2K4	SH3KBP1
LIN28B	TFRC	MAP3K1	SHC1
MAX	TK1	MAPK1	SNAI1
MINA	TP53	MAPK3	SOS1
MMP9	TRRAP	MAPK8	SRC
MTA1	UBTF	MET	WASL

Title: FGF signaling controls liver size in humanized chimeras

Supplemental Figure Legends

Supplemental Figure 1: Insertion of human DNA into mouse genome. (**a**) Bacterial artificial chromosome (BAC) RP11-266K14 with ~164 kb human DNA (chromosome 11) with genomic FGF19 sequence in the middle was introduced as a transgene into FRGN mice. A strategy using different PCR primer pairs was used to confirm the presence of the entire BAC in the transgenic mouse. (**b**) Example of PCR used to confirm presence of human DNA presence in transgenic mouse genome but not non-transgenic littermates. **(c)** Schematic view of the BAC used showing the relative positions of two other full coding sequences. **(d)** RNA sequence data showing RNA expression of the 3 human genes contained within the BAC in 3 conditions. Also shown are the orthologous murine genes in the transgenic and non-transgenic mice in the noted conditions. For the control and bile duct ligation (BDL) data, one transgenic and one non-transgenic mouse was used for each dataset. For the repopulated data, 3 mice for each genotype was used.

Supplemental Figure 2: DNA replication, cell cycle, apoptosis transcription pathways. Analysis of transcriptional pathways from RNA sequencing data (human transcriptome only) from liver tissue of human hepatocyte repopulated mice, either FR19- (n = 3) or FRGN19+ (n = 3) mice; statistics generated through GSEA showed that DNA replication and cell cycle pathways were significantly activated in repopulated livers of FRGN19- compared to FRGN19+ mice, while there was no difference in apoptosis-associated gene expression.

Supplemental Figure 3: Liver growth and regeneration transcription pathways. Analysis of transcriptional pathways from RNA sequencing data (human transcriptome only) from liver tissue of human hepatocyte repopulated mice, either FRGN19- (n = 3) or FRGN19+ (n = 3) mice; statistics generated through GSEA showing that the FOXM1 transcription pathway was significantly activated in repopulated livers of FRGN19- compared to FRGN19+ mice, while there were no significant differences other pathways commonly associated with liver growth and regeneration. Western blotting for FoxM1 protein showed that FoxM1 was mildly elevated in FRGN19- fully repopulated mice, but not significantly detected in fully repopulated FRGN19+ mice. FoxM1 was significantly expressed in "Actively Repopulating" livers (2 months

after human hepatocyte transplantation, prior to full repopulation) in mice of both genotypes (each lane represents a different mouse).

Supplemental Figure 4: RNA sequence data from human hepatocytes in FRGN and FRGN19+ mice. Depictions of single gene expression from RNA sequence data of single-donor human hepatocyte repopulated FGRN19- or FGRN19+ mice (n = 3 each); comparison made to human liver tissue (n = 1) and isolated human hepatocytes (n = 1); statistics (two-tailed t-test) compare only the transplanted human hepatocytes (n = 3 each). Y axix refers to Reads Per Kilobase Million (RPKM), used to normalize samples. The TGR5 graph under "Bile acid metabolism" also includes RNA sequence data from one gallbladder from an FRGN19+ mouse that had undergone BDL for 7 days.

Supplemental Figure 5: Subset of genes in the whole liver (a) and intestine (be) from mice with PV infusion of bile acids showing normal physiological response to excess bile acids in both tissues.

S1 Generation of transgenic mice with human FGF19

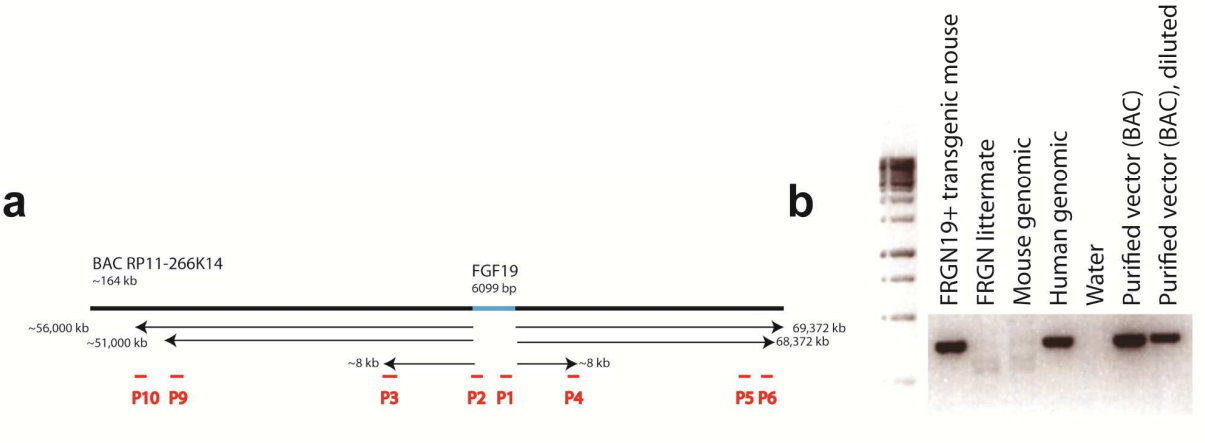

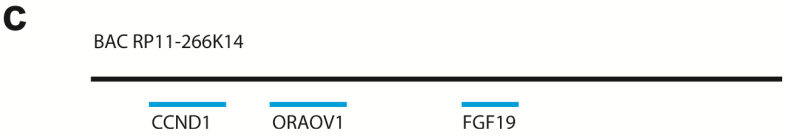

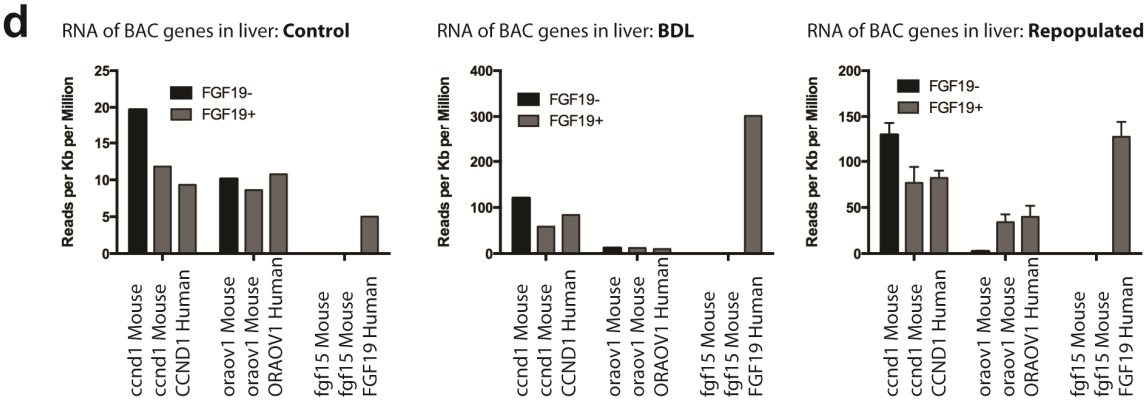

S2 DNA replication, cell cycle, apoptosis transcription pathways

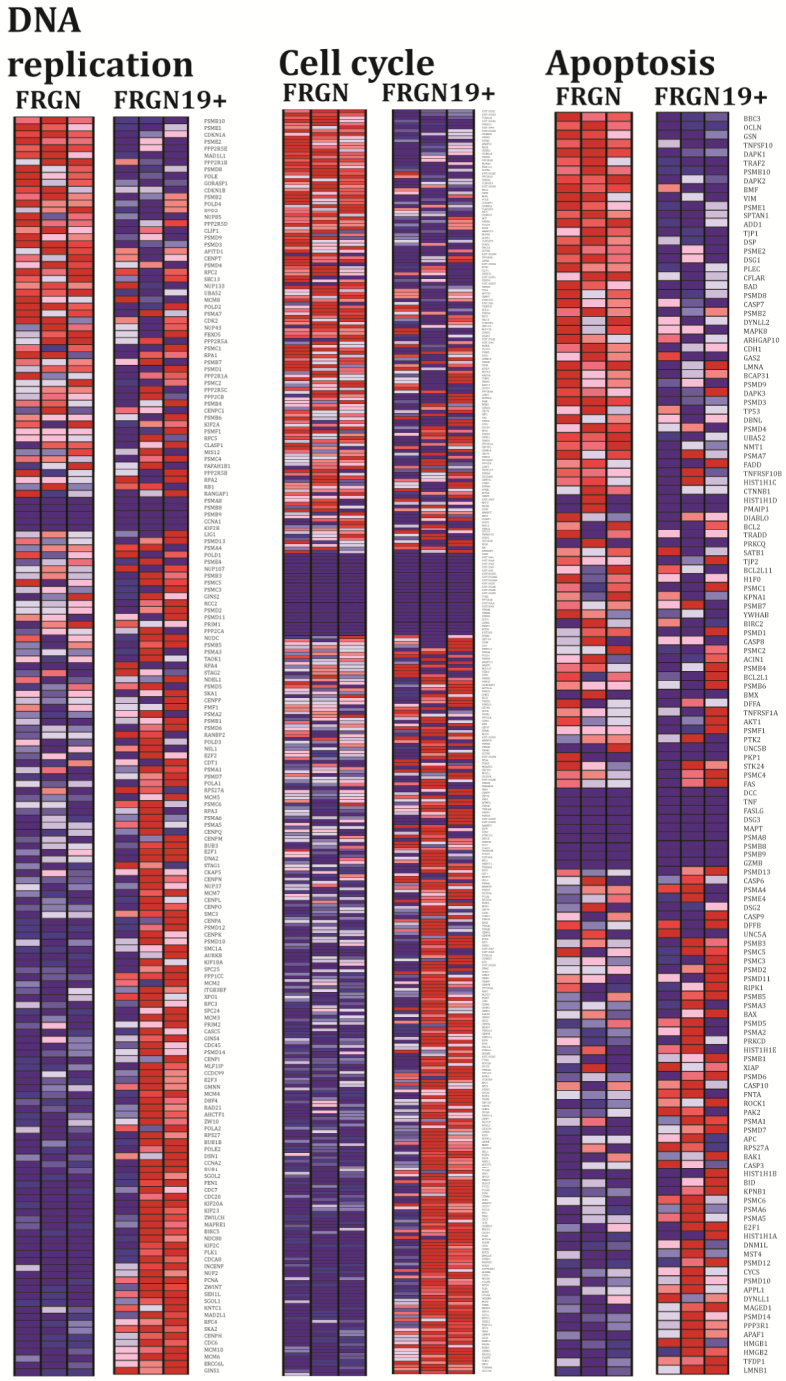

Nominal p value <0.001
FDR q-value <0.001

Nominal p value <0.001
FDR q-value =0.002

Nominal p value =0.380
FDR q-value = 0.774

S3 Liver growth and regeneration transcription pathways

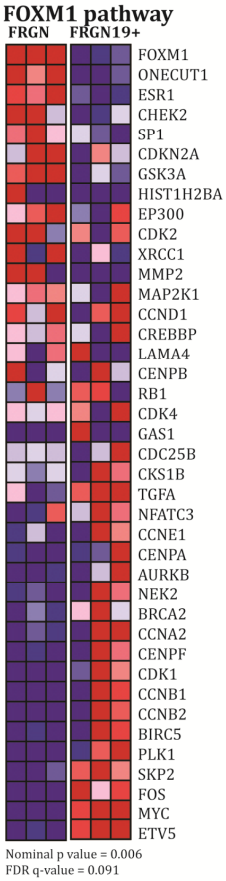

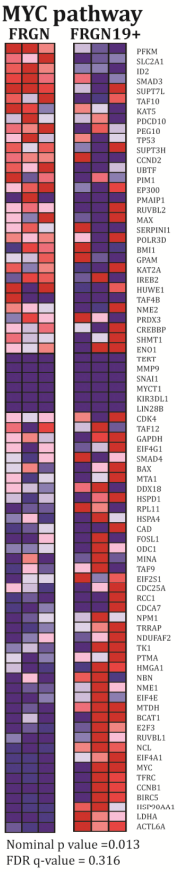

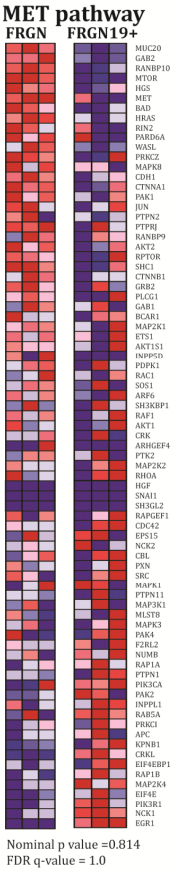

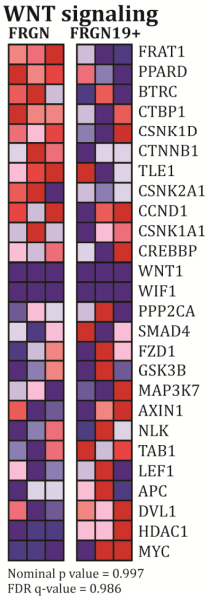

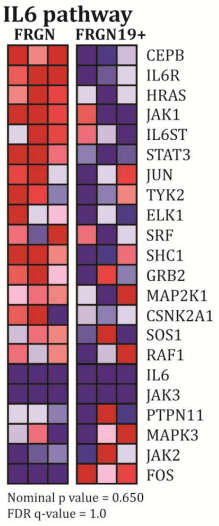

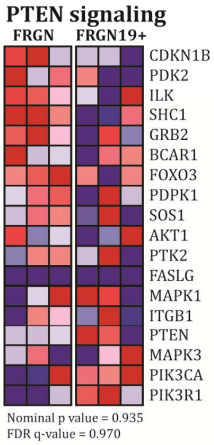

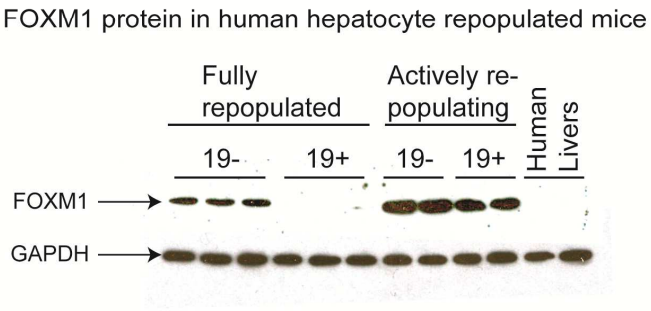

S4 RNA sequence data from human hepatocytes in FRGN and FRGN19+ mice

a Bile acid metabolism

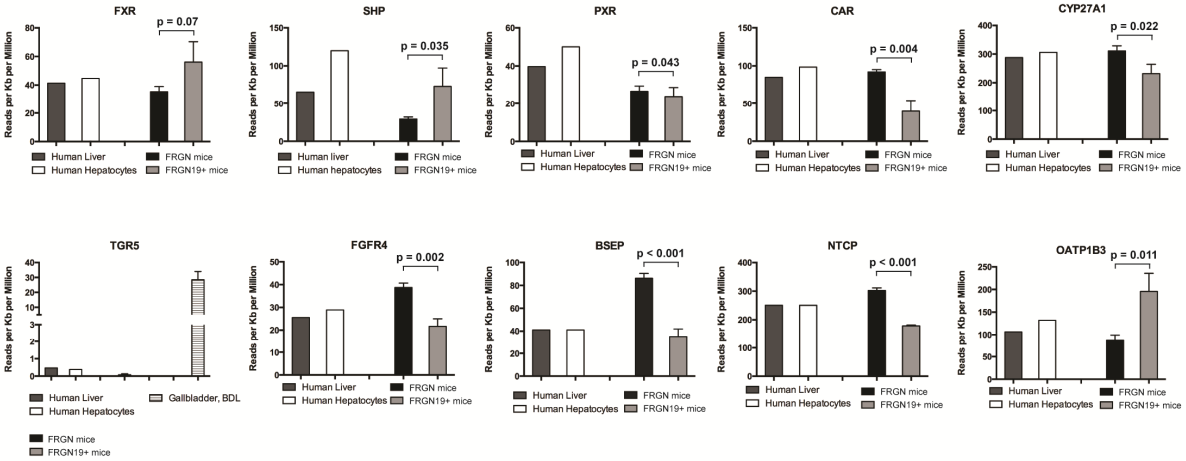

b Lipoprotein metabolism

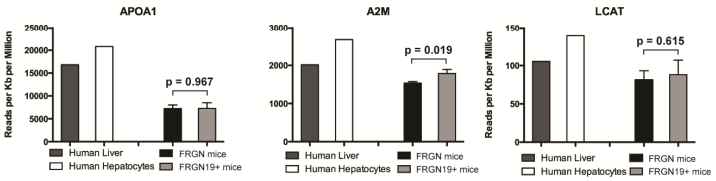

c Amino acid metabolism

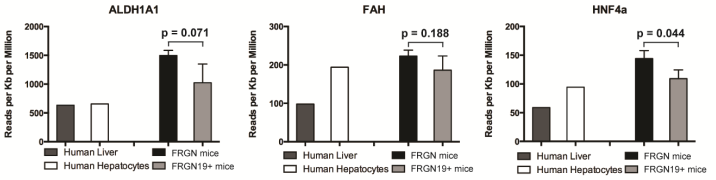

d Glucose metabolism

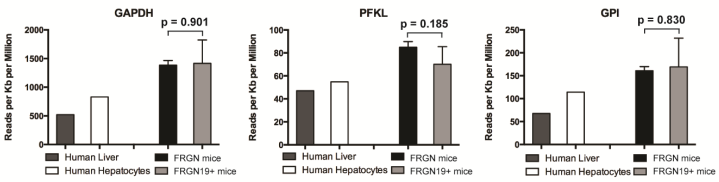

e Coagulation

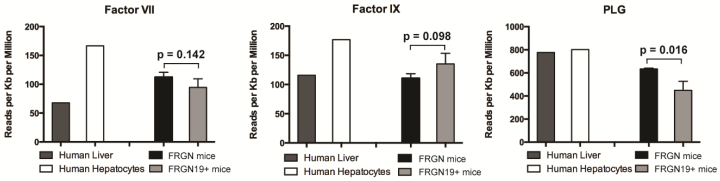

f Drug metabolism

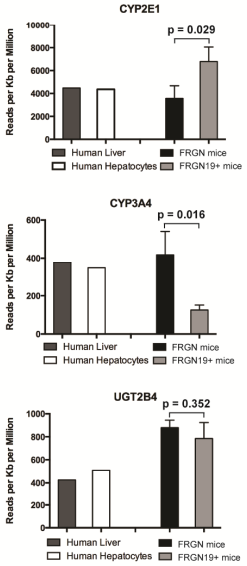

S5 Normal physiological response to bile acids in FRGN19+ mice

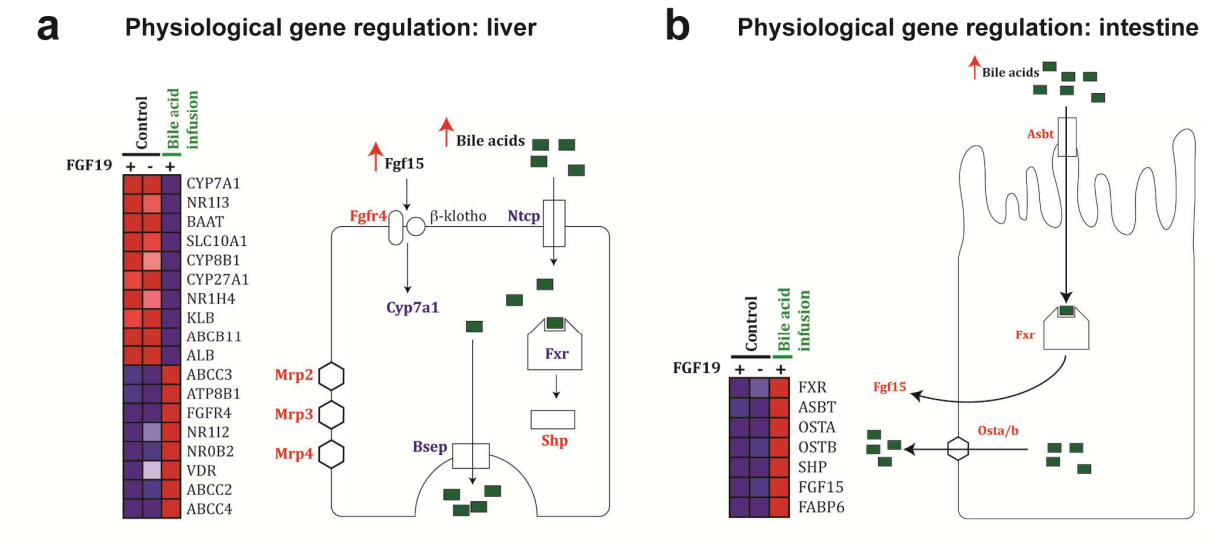

S6 Physiologic compartments of bile acid pool

a Portal vein bile acid concentration

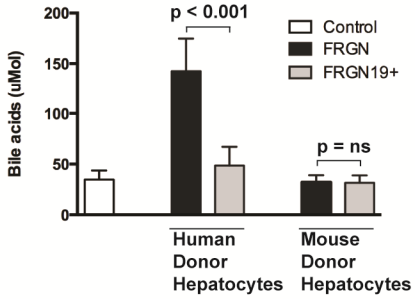

b Systemic bile acid concentration

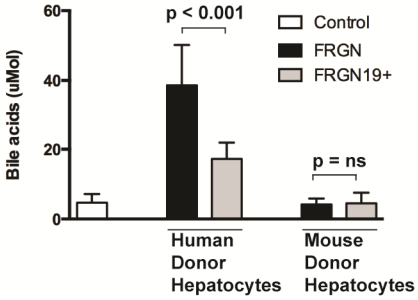

c Hepatic bile acid concentration

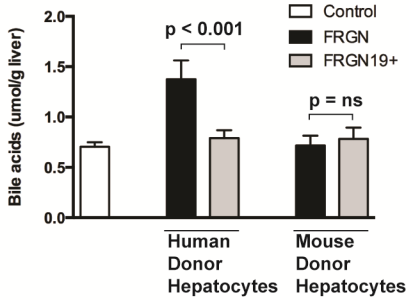

S7 Bile acid activation upstream of YAP signaling

a IQGAP1 in mice with bile acid excess